CLASSIFICATION CANCELLED

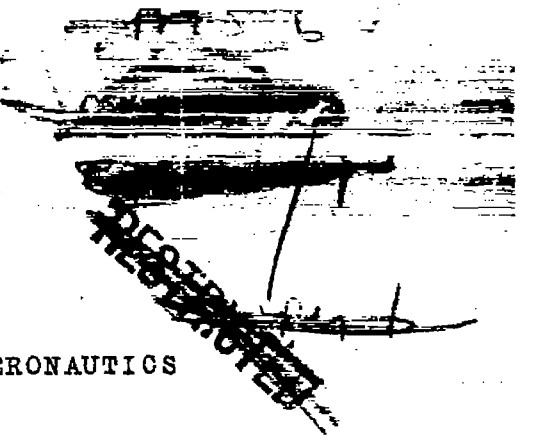

TECHNICAL NOTES

NATIONAL ADVISORY COMMITTEE FOR AERONAUTICS

No. 836

HYDRODYNAMIC TESTS OF A 1/10-SIZE MODEL OF THE HULL OF THE LATÉCOÈRE 521 FLYING BOAT - NACA MODEL 83

By Roland E. Olson and Lindsay J. Lina
Langley Memorial Aeronautical Laboratory

CLASSIFIED DOCUMENT

This document contains classified information affecting the National Defense of the United States within the meaning of the Espionage Act, USC 50:31 and 32. Its transmission or the revelation of its contents in any manner to an unauthorized person is prohibited by law. Information so classified may be imparted only to persons in the military and naval Services of the United States, appropriate civilian officers and employees of the Federal Government who have a legitimate interest therein, and to United States citizens of known loyalty and discretion who of necessity must be informed thereof.

Washington
December 1941

NASA Technical Library
3 1176 01425 7365

NATIONAL ADVISORY COMMITTEE FOR AERONAUTICS

TECHNICAL NOTE NO. 836

HYDRODYNAMIC TESTS OF A 1/10-SIZE MODEL OF THE HULL OF THE LATÉCOÈRE 521 FLYING BOAT - NACA MODEL 83

By Roland E. Olson and Lindsay J. Lina

SUMMARY

A 1/10-size model of the hull of the French flying boat Latécoère 521 was tested in the NACA tank. This model is one of a series of models of the hulls of actual flying boats of both foreign and domestic type that are being tested in the NACA tank to provide information regarding the water characteristics of a variety of forms of hull and to illustrate the development of present-day types of flying boat. The lines and the offsets of the hull were obtained from the manufacturer through the Paris Office of the NACA. The form of the stub-wing stabilizers was not furnished and, therefore, the model was tested without them.

The model was tested free to trim at the design initial load (initial load coefficient of 0.428) and by the general method at load coefficients from 0.025 to 0.6. The spray characteristics of the model are good. (The form of the bow would be particularly desirable for rough-water use. The interference of the afterbody and the tail extension is excessive, causing very high resistance at high speeds. A violent vertical instability is present at trims of 4° and 6° with light loads and high speeds.)

INTRODUCTION

Tests of models of hulls of successful flying boats are included in the program of research conducted at the NACA tank (references 1 to 8). The results of these tests are intended to provide information regarding the water characteristics of a variety of forms of hull and to illustrate the development of present-day types of flying boat.

The subject tests were made on a model of the hull of the flying boat Latécoère 521 ("Lt. de Vaisseau de Paris"), designated NACA model 83. This flying boat, which was built in France in 1934 and which at one time held the long-distance record for flying boats, was constructed primarily for trans-Atlantic operation.

The lines and offsets of the hull were furnished by the manufacturers through the Paris Office of the NACA. Data for the stub-wing stabilizers were not included in the data furnished to the NACA; consequently, the tank model did not have stub-wing stabilizers.

These tests of the hull without the stub-wing stabilizers are of special interest because the form of the hull differs from that generally used on American flying boats. It has a rounded bottom instead of the usual sharp keel; the main step is extremely shallow and of unusual form; and the angle of afterbody keel is very small.

DESCRIPTION OF THE MODEL

The model, 1/10-full size, was built of laminated wood according to the lines shown in figure 1 and the offsets given in table I. Photographs of the model are shown in figure 2.

The model has a relatively long forebody with the keel carried low and well forward and with sharp V sections at the bow. The angle of dead rise at the main step is 20° 15' and the bottom sections are arched to give a large chine flare. The keels of the forebody and the afterbody are transversely rounded, as in NACA model 74 (reference 9), but a sharp keel is formed near the bow and near the second step. The angle of dead rise on the afterbody increases toward the stern post. Chine flare is also used on the afterbody bottom just aft of the main step. The tail appendage has straight V sections with no curvature at the chine.

The main step is shallow (0.37 in., 0.021 beam) and is not vertical, as in American designs, but slopes aft from the forebody to the afterbody. The second step (0.46 in.) fades out at the chine and also slopes toward the tail extension. (See fig. 1.)

The angle of afterbody keel is 2° 11' with respect to the straight portion of the forebody. The keel of the tail extension is straight and at an angle of 12° 48' with respect to the forebody.

The lateral stability of the full-size flying boat was provided by stub wings attached to the hull. Lack of information as to the size and the form of the stub wings prevented their being used on the model.

The particulars of the model and of the full-size flying boat are as follows:

	Model	Full-size
Length:		
Over-all	116.65 in.	97.21 ft
Forebody	54.53 in.	45.44 ft
Afterbody	26.37 in.	21.98 ft
Tail extension	35.75 in.	29.79 ft
Maximum beam	17.72 in.	14.77 ft
Center of moments:		
Forward of main step	7.48 in.	6.23 ft
Above keel	12.80 in.	10.67 ft
Depth of main step	0.37 in.	0.31 ft
Depth of second step at keel	0.46 in.	0.38 ft
Angle of afterbody keel	2° 11'	
Angle of tail-extension keel	12° 48'	
Gross load	87.4 lb	88,184 lb
Get-away speed	37.5 fps	80.8 mph
Linear ratio of model to full size	1/10	

Additional tests of the model were made with the tail extension removed at the second step. For this portion of the investigation, the model was designated model 83A.

APPARATUS AND PROCEDURE

A detailed description of the tank, the towing equipment, and the method of testing are given in reference 10. The model was tested, free to trim, at one gross load and one get-away speed. Fixed-trim tests were made by the general method. Inasmuch as the investigation was intended to study the behavior of the hull rather than to provide design data, the tests did not include all possible conditions of operation.

The position of the center of gravity of the complete flying boat as shown on the original lines was used as the center of gravity for the free-to-trim tests and the center of moments for the fixed-trim tests. The free-to-trim tests of the model with tail extension removed (model 83A) were made with the model balanced about the center of gravity by placing weights on the afterbody. The proper load on the water was also maintained.

Photographs were taken for a qualitative record of the wave form and the spray characteristics.

RESULTS AND DISCUSSION

The results of the tests were reduced to the usual coefficients based on Froude's law in order to make them independent of size. In this case, the maximum beam was chosen as the characteristic dimension. The nondimensional coefficients are defined as follows:

Load coefficient, $C_{\Delta} = \Delta/wb^3$

Initial load coefficient, $C_{\Delta_o} = \Delta_o/wb^3$

Resistance coefficient, $C_R = R/wb^3$

Speed coefficient, $C_V = V/\sqrt{gb}$

Get-away speed coefficient, $C_{V_G} = V_G/\sqrt{gb}$

Trimming-moment coefficient, $C_M = M/wb^4$

Rise coefficient, $C_r = r/b$

where

Δ load on water, pounds

Δ_o initial load on water, pounds

w specific weight of water, pounds per cubic foot (63.4 for these tests, usually taken as 64 for sea water)

b maximum beam, feet

R water resistance, pounds

V speed, feet per second

V_G get-away speed, feet per second

g acceleration of gravity, 32.2 feet per second per second

M trimming moment, pound-feet

r rise at center of gravity (height above position at rest), feet

Any consistent system of units might have been used. The trimming-moment data are referred to the center of moments shown in figure 1. Tail-heavy moments are considered positive. Trim (τ) is the angle between the base line of the model and the horizontal.

Free to trim, model 83.- The results of the free-to-trim tests for the design condition of loading (C_{Δ_o} = 0.428) and get-away speed (C_{V_G} = 5.50) are plotted in figure 3. The photographs in figure 4 show the spray pattern at typical speeds.

The wave formation and the spray at low speeds are shown in figure 4(a). The fine entrance resulting from the low keel and the sharp sections at the bow produces only a low spray, and the flying boat will probably run very cleanly in rough water. This low spray may be due in some extent to the unusually low load coefficient at which the test was made. The tests of the model show no indication of any lateral instability when the flow breaks away from the after portion of the hull at low speeds.

The maximum in the resistance curve (the hump) occurs at a speed coefficient of 2.4. At the speed represented by this coefficient, the model planes on the forebody and the afterbody and the tail extension is still wetted by spray from under the second step. The small angle of afterbody keel is effective in keeping the trim at the hump at the low value of only 7.3°. The load-resistance ratio Δ/R at the hump is about 5. This rather high value of Δ/R for a free-to-trim test may be accounted for by the fact that the attitude of the hull is near the trim for minimum water resistance (best trim) at this speed. Photographs (fig. 4(b)) show the wave pattern at the hump speed. The forward portion of the spray from the forebody is low and almost horizontal.

Over the hump, the trim and the resistance decrease slightly and the afterbody and tail extension are clear for only a limited range of speeds. The model had a slight tendency to porpoise as the afterbody came clear, but readings of resistance, trim, etc. could be made without restraining the model in pitch.

At high speeds the trim increases, resulting in a large departure from trim for minimum water resistance (see fig. 6(b)) and a second hump occurs in the resistance curve. The low angle of afterbody keel and the shallow step do not provide clearance for the afterbody, and the after planing surfaces are heavily wetted near get-away speed (fig. 4(c)). The shallow second step, which fades out at the chines, is ineffective in breaking the flow from the tail extension.

Free to trim, model 83A (tail extension removed).- The free-to-trim curves for model 83A are included in figure 3 with the free-to-trim curves for model 83.

Below the hump speed, the resistance and the trim for model 83A are greater than for model 83. This result indicates that at low speeds the tail extension of model 83 produces an effective lifting force and causes a greater positive (bow up) moment. The hump is shifted to a lower speed ($C_V = 2.0$) but the magnitude of the hump resistance is not changed. At high speeds the trim and the resistance for model 83A are reduced, showing that, in model 83, the tail extension produces a downward force causing higher trim and resistance. The same hump in the resistance curve at high speeds occurs for model 83A but to a lesser degree.

Fixed-trim tests.- The fixed-trim results for the model with the tail extension are presented in figure 5. The resistance coefficients for a series of loads are plotted against the speed coefficient for several trims. A few cross plots of the type generally used by the NACA are included in figure 6. The use of these curves is described in reference 8.

The resistance characteristics of model 83 are somewhat different from those of most models tested in the NACA tank. Instead of an appreciable decrease in resistance just beyond the hump speed, which is generally associated with a decrease in wetted area over the after portion of the hull, the resistance remains practically the same ($\tau = 6^\circ$ or $\tau = 8^\circ$) or continues to increase ($\tau = 10^\circ$). With the low angle of afterbody keel and the shallow step, the after planing surfaces are in such a position that the water from the main step generally will not clear the afterbody. With the heaviest loads, however, the trough formed by the forebody is deep and for a very small range of speeds the afterbody and the tail extension are clear of the water. At low angles and high speeds the resistance is high because the wetted length forward of the step increases and more than compensates for any reduction in afterbody interference. At a trim of 10° the light loads are supported by the after planing surfaces.

Figures 7(a) to 7(c) show the spray at a fixed trim of 8° for three loads and speeds. At low speed, $C_V = 1.30$ and $C_\Delta = 0.4$, the sides of the model are wetted and the tail deck is almost under water (fig. 7(a)). As the speed increases over the hump the afterbody tends to clear, but a further increase in speed causes the water

from the main step again to strike the afterbody chines (fig. 7(b)). For the light loads the main step is very ineffective in breaking the flow from the afterbody and as a result the afterbody just behind the step is wetted. At high speeds (fig. 7(c)) the afterbody and the tail extension are heavily wetted.

Best trim.- The force characteristics at trim for minimum water resistance are given in figure 8.

Vertical instability.- At high speeds and light loads a violent vertical instability was evident at trims of 4° and 6°. The model appeared to be sucked down into the water until the flow changed and sufficient lift was developed to cause the model to jump completely clear of the water. This same type of instability was noted for tests reported in reference 9. These and other tests indicate that the instability appears when the step is not of sufficient depth. The instability occurs over a range of trims of several degrees. The instability does not appear at 2°, where the afterbody keel is slightly above the horizontal.

The instability prevented complete data being taken at high speeds for the light loads. The free-to-trim tests did not show this characteristic because the trim, throughout the high-speed range, was above that at which the vertical instability occurred. (See fig. 6(b).)

The effect of this type of vertical instability on porpoising characteristics should be investigated by use of a dynamically similar model; that is, a model with the mass and moment of inertia corresponding to the full-size airplane. No information has been received on the corresponding behavior of the full-size flying boat.

Sticking.- At trims of 6° and 8° (model 83) the moments change from negative (bow down) to positive (bow up) values at high speeds. A change of moment in this direction does not occur in most models at high speeds. This change of moment indicates that the model is probably sticking because of the flow over the after planing surfaces.

The resistance and moment coefficients for model 83A (tail extension removed), at a trim of 8°, are shown in figure 9. With the tail extension removed, the moments become and remain negative at high speeds. When figure 5(d) (model 83) is compared with figure 9 (model 83A),

the difference in moments indicates that a downward, or suction, force is developed at high speeds because of the presence of the tail extension. Photographs in figure 7 show an increase in wetted area forward when the tail extension is present.

In figure 10 the position, the magnitude, and the direction of the resultant force are shown at several loads and speeds for model 83 and model 83A. The trim of the hull is 8°. These vectors were computed from the fixed-trim data.

At low speeds (C_V = 2.0) the position of the resultant force (fig. 10) is farther aft for model 83 (with the tail extension), indicating a lifting force over the planing surface of the tail extension. (Note the roach in the low-speed photographs, figs. 7(a) and 7(b).) As the tail extension tends to come clear of the water (C_V = 3.0) the force vectors for the two models approach one another. As the speed increases, the water again flows over the tail planing surface (model 83, figs. 7(b) and 7(c)), and the resultant force moves forward with decreasing slope. The vectors for model 83 at speed coefficients from 4.5 to 7.0 show the resultant force intersecting the forebody; whereas the resultant force for model 83A intersects the afterbody at all loads except C_Δ = 0.1.

CONCLUSIONS

Because of the absence of the stub wings, the characteristics of the model are not completely indicative of the performance of the full-size flying boat.

The spray characteristics of the hull are good, but this result may be due in some extent to the unusually low load coefficients at which the tests were made. On the basis of water performance, the form of the bow appears to be good. The chine flare is effective in holding down the spray.

Because of the low angles of afterbody keel and tail extension, a lift is produced at low speeds that is advantageous in reducing the trim at the hump where the available control moment is small.

The high-speed resistance is excessive because of the lack of clearance in the afterbody and tail extension.

At fixed trims of 4° and 6° a violent vertical instability appears at light loads and high speeds. This instability is probably caused mainly by the shallow step. Knowledge of the full-scale behavior is desireble for interpretation of this type of instability.

Langley Memorial Aeronautical Laboratory,
National Advisory Committee for Aeronautics,
Langley Field, Va., October 13, 1941.

REFERENCES

1. Shoemaker, James M.: A Complete Tank Test of a Model of a Flying-Boat Hull - N.A.C.A. Model 16. T.N. No. 471, NACA, 1933.

2. Dawson, John R.: A Complete Tank Test of the Hull of the Sikorsky S-40 Flying Boat - American Clipper Class. T.N. No. 512, NACA, 1934.

3. Bell, Joe W.: Tank Tests of a Model of the NC Flying-Boat Hull - N.A.C.A. Model 44. T.N. No. 566, NACA, 1936.

4. Allison, John M.: Tank Tests of a Model of the Hull of the Navy PB-1 Flying Boat - N.A.C.A. Model 52. T.N. No. 576, NACA, 1936.

5. Dawson, John R., and Truscott, Starr: A General Tank Test of a Model of the Hull of the British Singapore IIC Flying Boat. T.N. No. 580, NACA, 1936.

6. Ward, Kenneth E.: Hydrodynamic Tests in the N.A.C.A. Tank of a Model of the Hull of the Short Calcutta Flying Boat. T.N. No. 590, NACA, 1937.

7. Allison, John M.: Tank Tests of a Model of One Hull of the Savoia S-55-X Flying Boat - N.A.C.A. Model 46. T.N. No. 635, NACA, 1938.

8. Dawson, John R.: A General Tank Test of a Model of the Hull of the P3M-1 Flying Boat Including a Special Working Chart for the Determination of Hull Performance. T.N. No. 681, NACA, 1938.

9. Truscott, Starr, Parkinson, J. B. Ebert, John W., Jr., and Valentine, E. Floyd: Hydrodynamic and Aerodynamic Tests of Models of Flying-Boat Hulls Designed for Low Aerodynamic Drag - N.A.C.A. Models 74, 74-A, and 75. T.N. No. 668, NACA, 1938.

10. Truscott, Starr: The Enlarged N.A.C.A. Tank, and Some of Its Work. T.M. No. 918, NACA, 1939.

TABLE I
MODEL 83 OFFSETS, INCHES

Station	Distance from F.P.	Distance from base line													Half-breadths			
		Keel	[a]B1 0.08	[a]B2 0.84	[a]B3 1.28	[a]B4 2.46	[a]B5 3.84	[a]B6 4.82	[a]B8 6.00	[a]B9 7.19	[a]B10 8.37	[a]B7 4.92	Chine	Deck	Chine	[b]WL1 10.04	[b]WL2 10.93	[b]WL3 11.61
F.P.	0.00												11.02	12.05	0.00	↑		
d	1.38	5.72	6.13	8.80									9.76		.84			
0	2.46	4.43	4.71	6.58	8.52								9.00	11.24	1.45			
a	3.74	3.58	3.70	5.16	6.74								8.27		2.13			
1	4.92	3.15	3.23	4.22	5.69	7.45							7.71	10.78	2.70			
2	7.38	2.49	2.51	3.10	4.15	5.85	6.76						6.82	10.45	3.77			
3	9.84	1.97	1.98	2.35	3.18	4.66	5.67						6.14	10.24	4.68			
5	13.27	1.41		1.61	2.18	3.44	4.49	5.11					5.39	10.09	5.75			
8	17.32	.91	.91	1.04	1.42	2.45	3.39	4.12	4.55				4.72	10.04	6.76			
12	22.05	.50	.50	.60	.91	1.75	2.59	3.33	3.85	4.11			4.17		7.66			
16	26.77	.23	.23	.31	.59	1.35	2.12	2.84	3.40	3.69			3.83		8.33			
19	30.61	.10	.10	.17	.43	1.16	1.90	2.61	3.17	3.48	3.60		3.62		8.64			
22	35.04	.02	.02	.09	.34	1.06	1.80	2.49	3.05	3.37	3.49		3.51		8.82			
25	39.57	.00	.00	.08	.33	1.05	1.78	2.48	3.03	3.34	3.44		3.45		8.86			
28	44.29	.00	.00	.08	.33	1.05	1.78	2.48	3.03	3.34	3.41		3.40		8.86			
31	49.02	.00	.00	.08	.33	1.05	1.78	2.48	3.03	3.33	3.37		3.34		8.86			
34	53.74	.00	.00	.08	.33	1.05	1.78	2.48	3.03	3.33	3.35		3.29		8.86			
35	54.53	.00	.00	.08	.33	1.05	1.78	2.48	3.03	3.33	3.34		3.28		8.85			
Step		.37	.37	.46	.74	1.48	2.22	2.93	3.50	3.89	4.08		4.12		8.85			
36	55.91	.41	.41	.50	.80	1.54	2.28	2.99	3.56	3.94	4.12	Deck for tail appendage	4.17		8.82			
38	58.46	.51	.51	.61	.94	1.71	2.46	3.19	3.77	4.15	4.33		4.36		8.72			
42	63.19	.69	.69	.84	1.20	2.03	2.82	3.57	4.18	4.56	4.75		4.75		8.38			
45	67.62	.86	.87	1.07	1.48	2.34	3.18	3.97	4.60	5.00			5.16		7.91			
48	72.05	1.03	1.05	1.33	1.79	2.69	3.57	4.40	5.06	5.54			5.60		7.33			
51	76.48	1.20	1.23	1.61	2.12	3.06	4.00	4.91	5.68				6.07		6.68			
54	80.90	1.38	1.45	1.92	2.47	3.49	4.50	5.52	6.54			11.19	6.54	10.04	6.00			3.54
Step		1.84	1.90	2.35	2.85	3.76	4.68	5.60	6.54				6.54	11.81	6.00			3.54
55	83.86	2.44	2.50	2.95	3.45	4.39	5.33	6.28				10.93	6.85		5.54			3.52
56	86.81	3.11	3.18	3.62	4.13	5.07	6.01	6.95				10.44	7.16		5.09		4.57	3.46
58	92.72	4.45	4.51	4.96	5.47	6.42	7.36						7.79		4.17		3.85	3.23
60	98.62	5.79	5.85	6.30	6.82	7.77							8.41		3.26		3.10	2.82
62	104.92	7.22	7.28	7.74	8.26								9.07		2.28		2.26	2.19
64	109.84	8.33	8.40	8.86	9.39								9.60		1.52		1.53	
66	114.76	9.45	9.51	10.01									10.12		.76		.76	
66a	115.25	9.56											10.17		.70			
66b	115.77	9.68											10.23		.57			
66c	116.29	9.80											10.28		.32			
A.P.	116.65	9.88											10.32	11.81	R=.10	↓		

Same as chine

[a]Distance of buttocks from center line.
[b]Distance of water line from base line.

National Advisory
Committee for Aeronautics

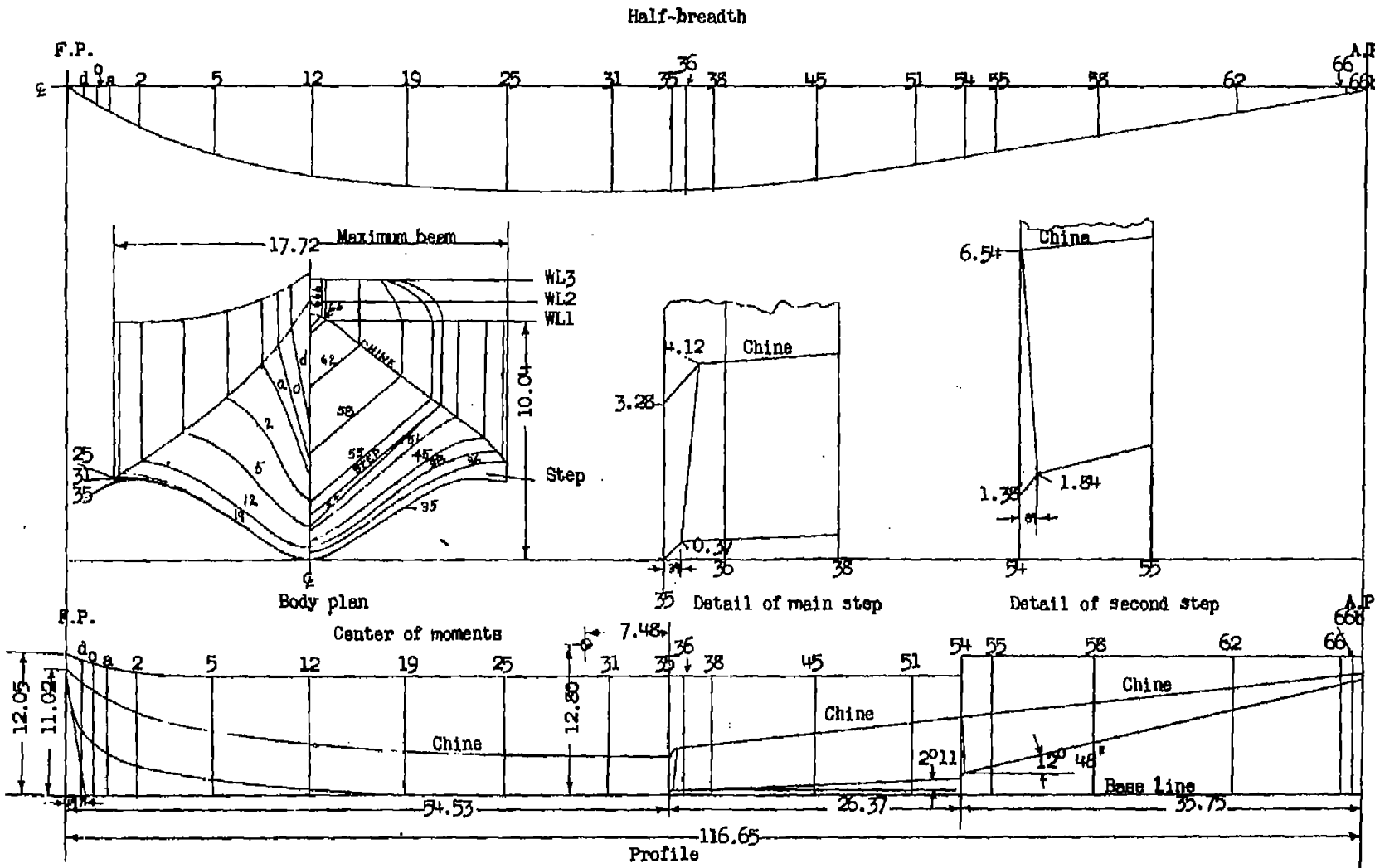

Figure 1.- Lines of NACA model 83.

Fig.1

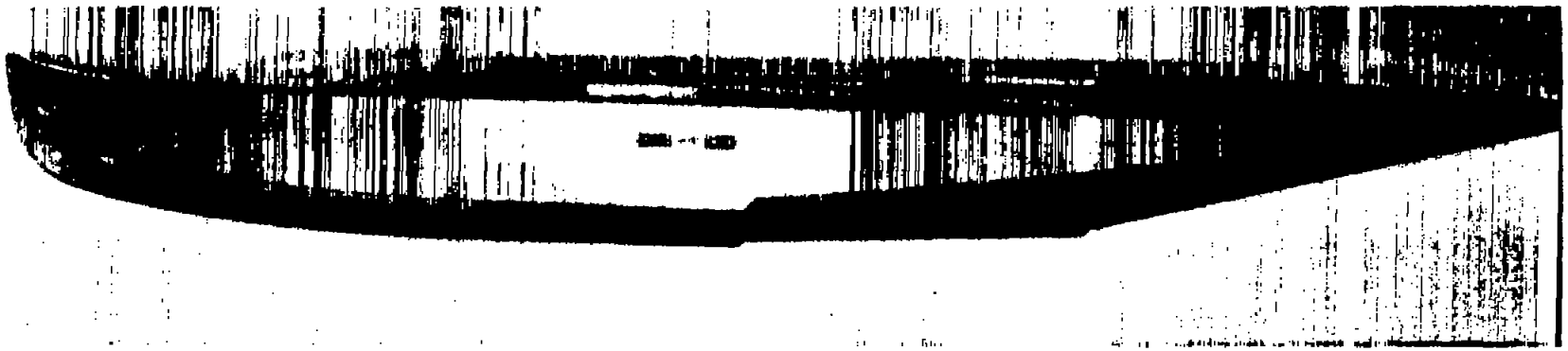

(a) Side view.

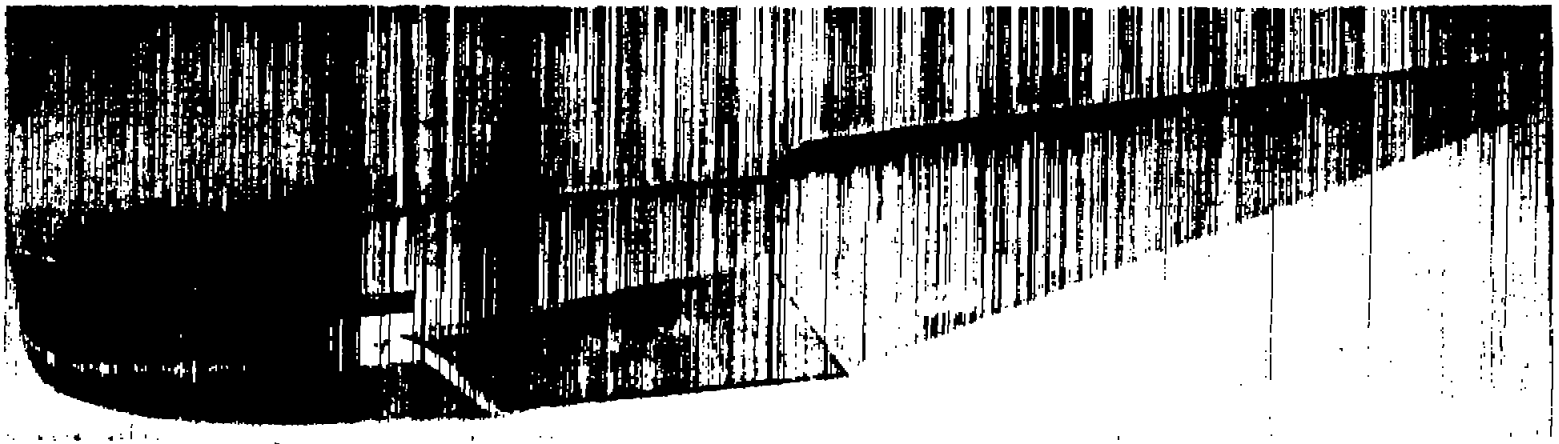

(b) Three-quarter view.

Figure 2.- NACA model 83.

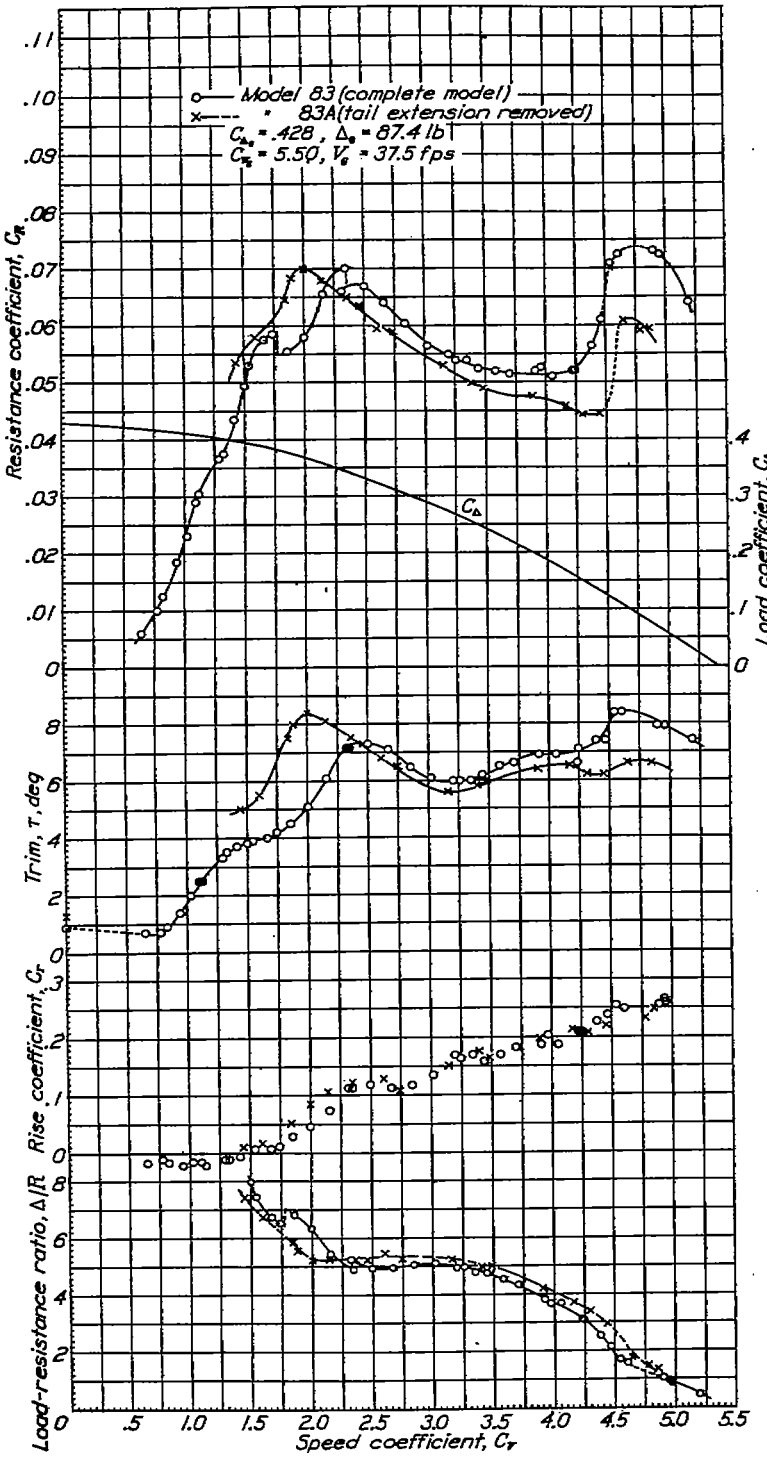

Figure 3.- Models 83 and 83A. Free-to-trim characteristics.

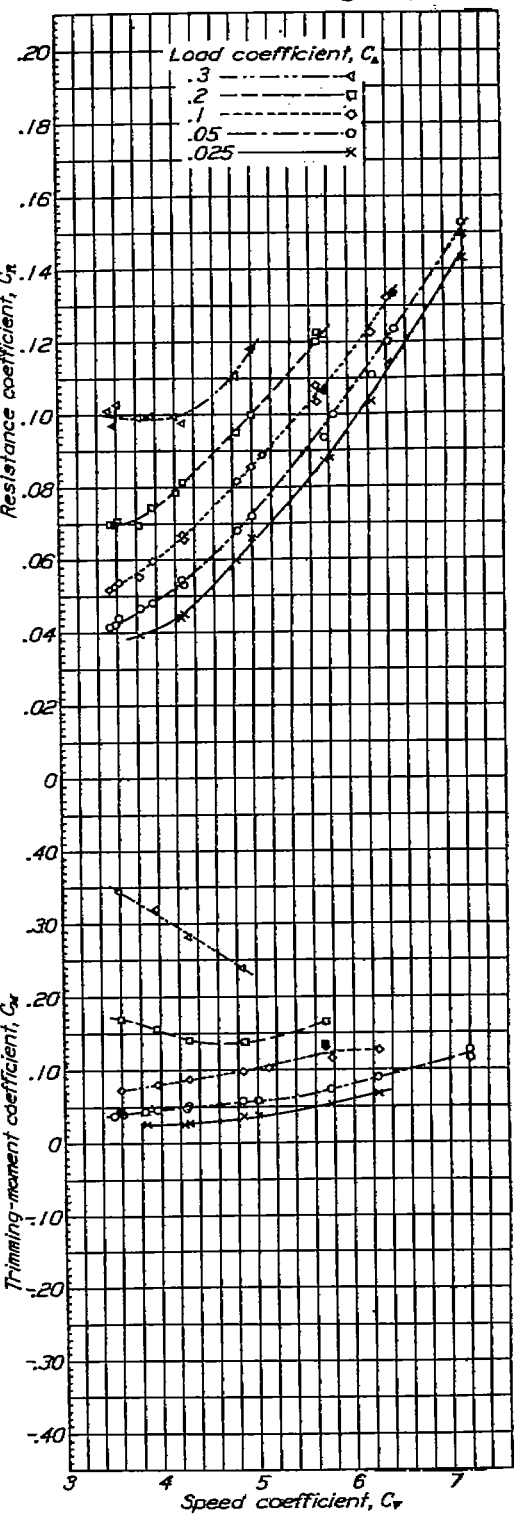

Figure 5(a).- Model 83. Resistance and trimming-moment coefficients, τ=2°.

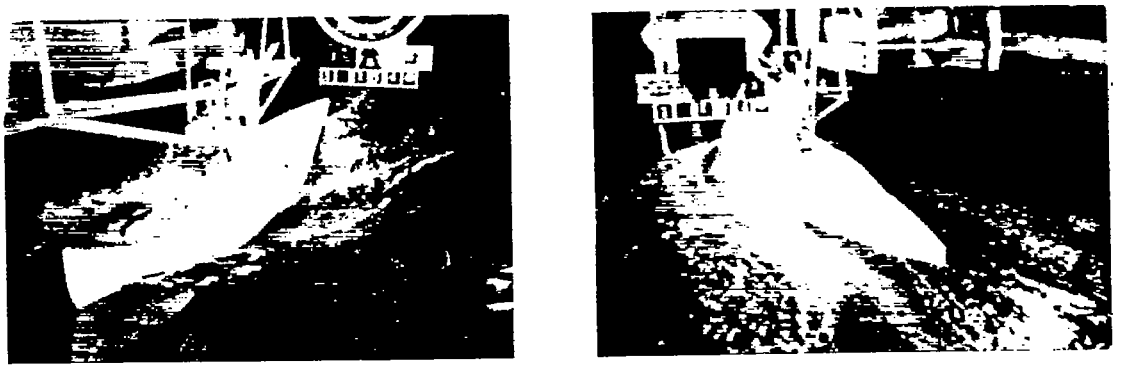

(a) $C_V = 0.80$, $\tau = 1.0^\circ$, $C_\Delta = 0.42$.

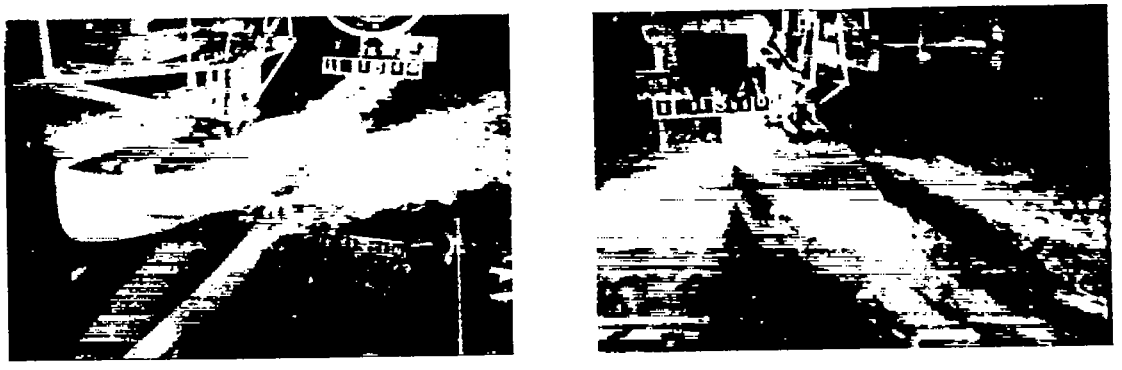

(b) $C_V = 2.35$, $\tau = 7.3^\circ$, $C_\Delta = 0.34$.

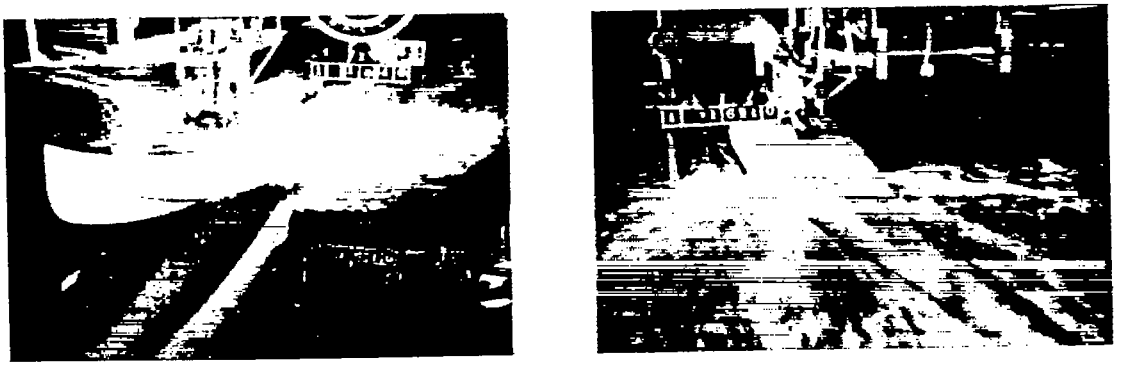

(c) $C_V = 4.60$, $\tau = 8.4^\circ$, $C_\Delta = 0.11$.

Figure 4.- Model 83. Free-to-trim.

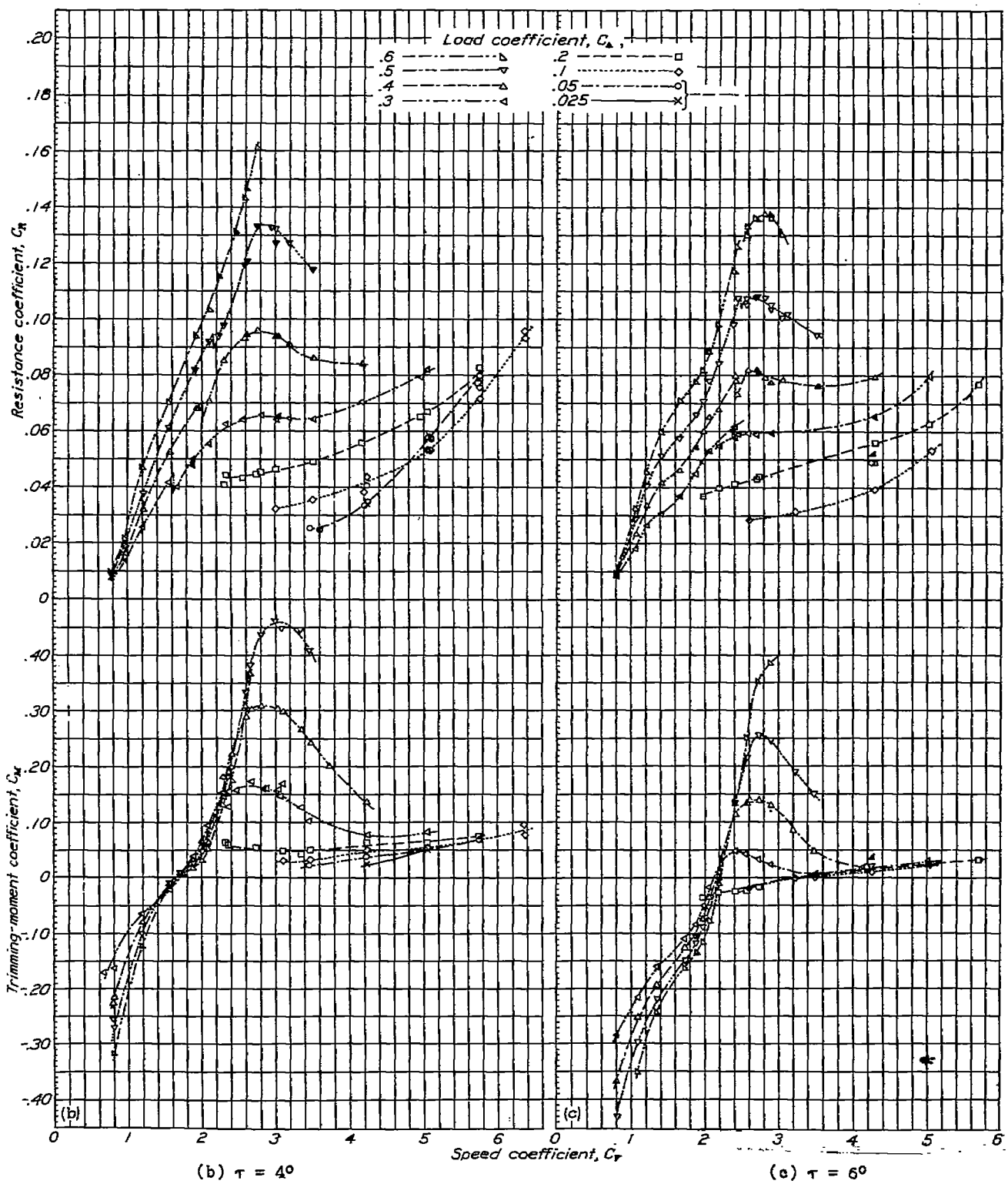

(b) $\tau = 4°$ (c) $\tau = 6°$

Figure 5(b,c).- Resistance and trimming-moment coefficients.

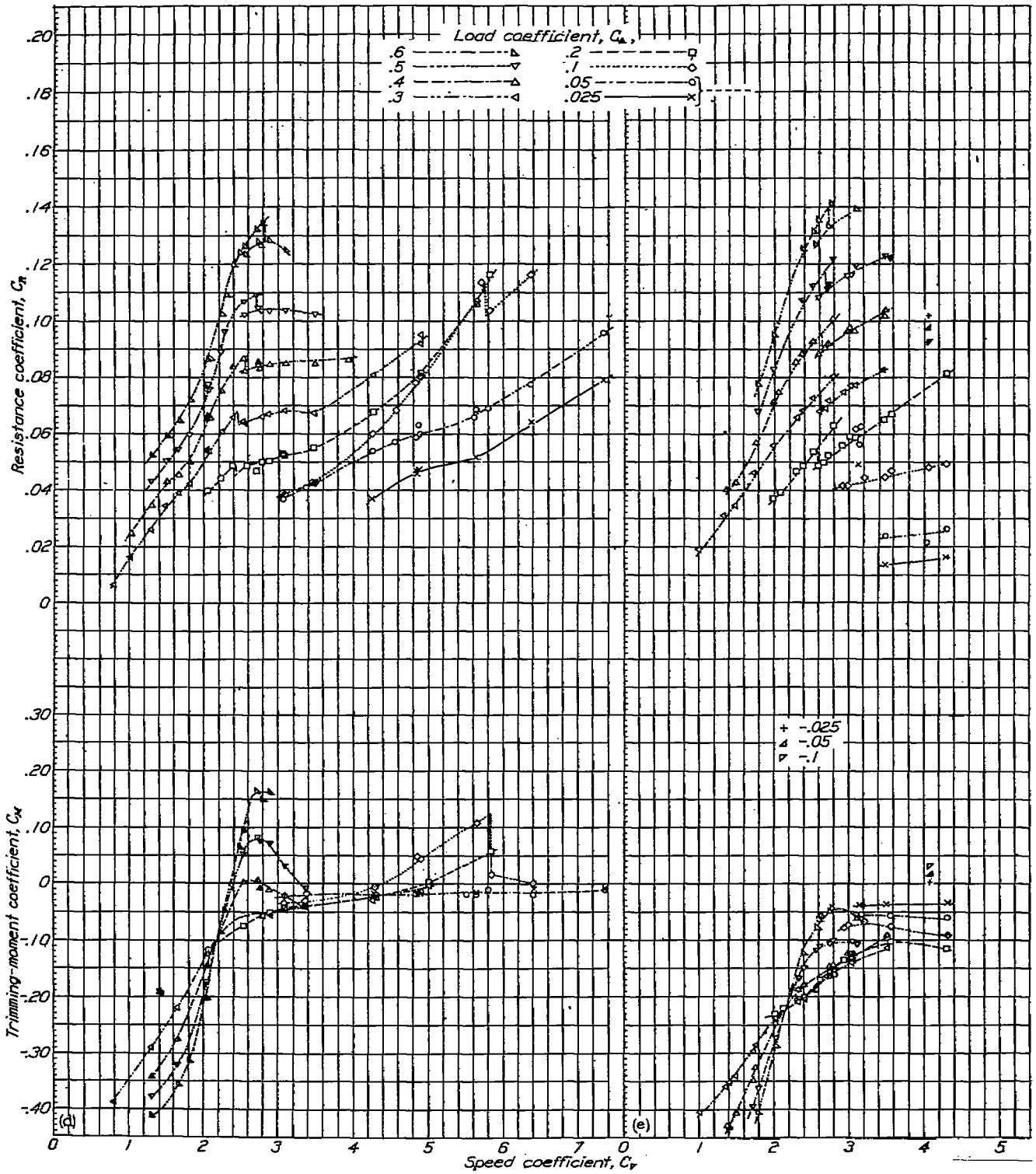

(d) $\tau = 8^\circ$ (e) $\tau = 10^\circ$

Figure 5(d,e).- Model 83. Resistance and trimming-moment coefficients.

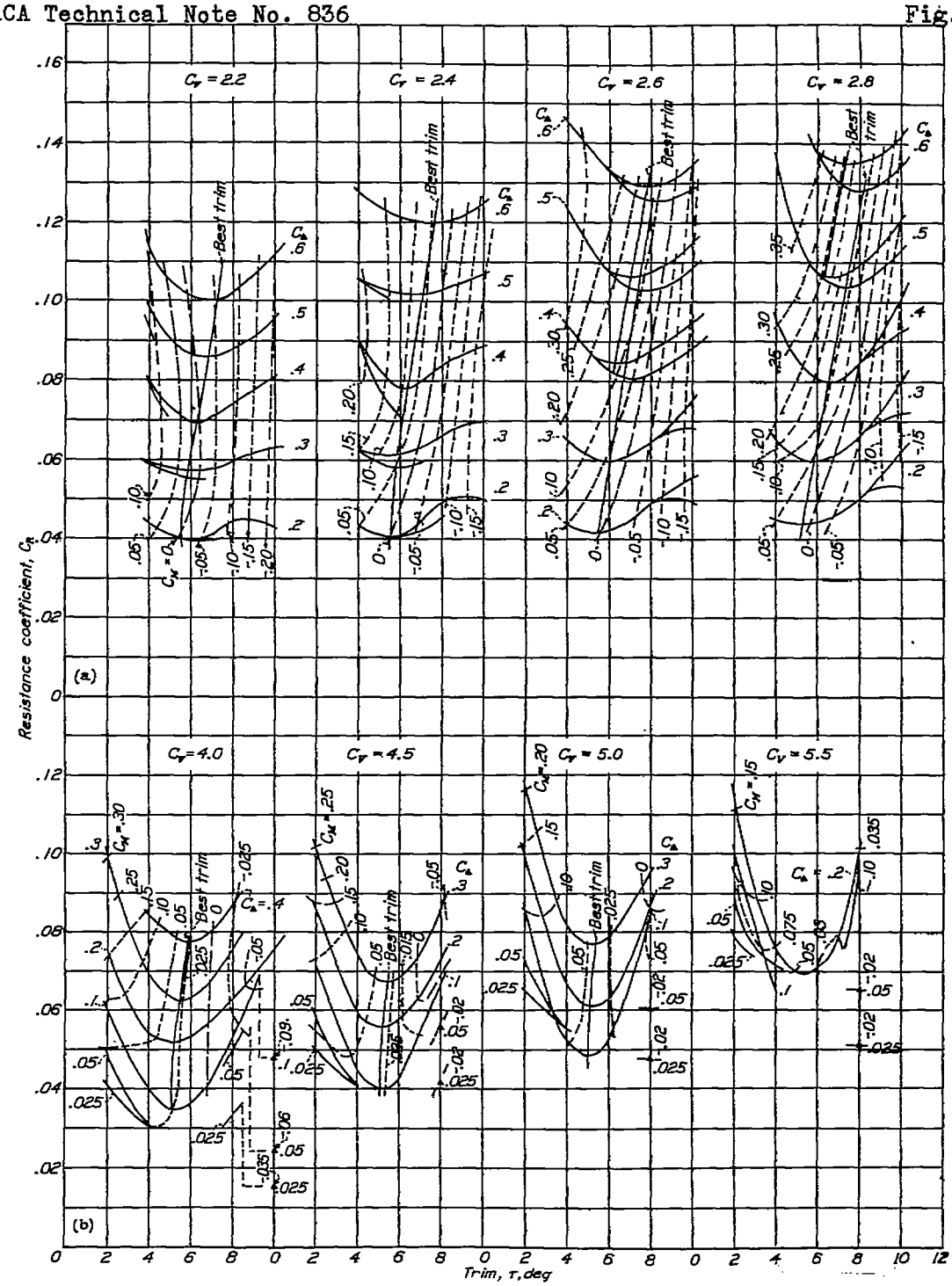

(a) Near hump speed.
(b) At high speeds.

Figure 6.- Model 83. Variation of resistance and trimming-moment coefficients.

(a) $C_{\Delta} = 0.4$, $C_V = 1.30$.

(d) $C_{\Delta} = 0.4$, $C_V = 1.30$.

(b) $C_{\Delta} = 0.05$, $C_V = 4.90$.

(e) $C_{\Delta} = 0.05$, $C_V = 5.10$.

(c) $C_{\Delta} = 0.05$, $C_V = 7.40$.

Model 83

(f) $C_{\Delta} = 0.05$, $C_V = 7.40$.

Model 83A

Figure 7.- Model 83 and 83A. Fixed trim. $\tau = 8^{\circ}$.

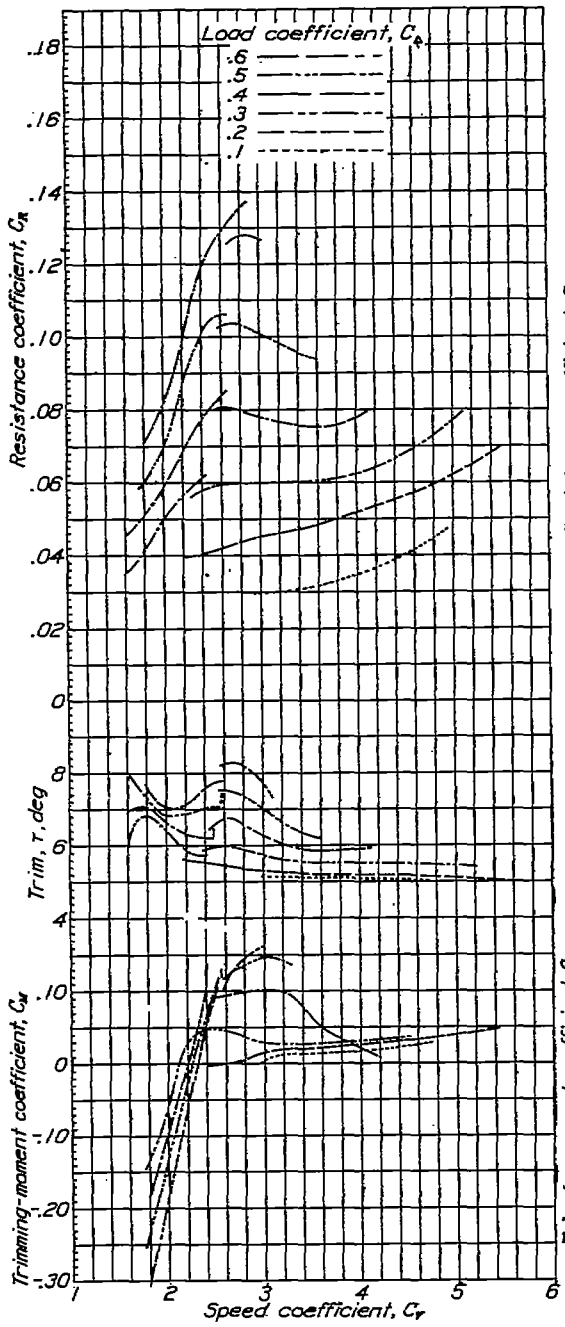

Figure 8.- Model 83. Variation of resistance, trim, and trimming moment at trim for minimum water resistance. (Best trim)

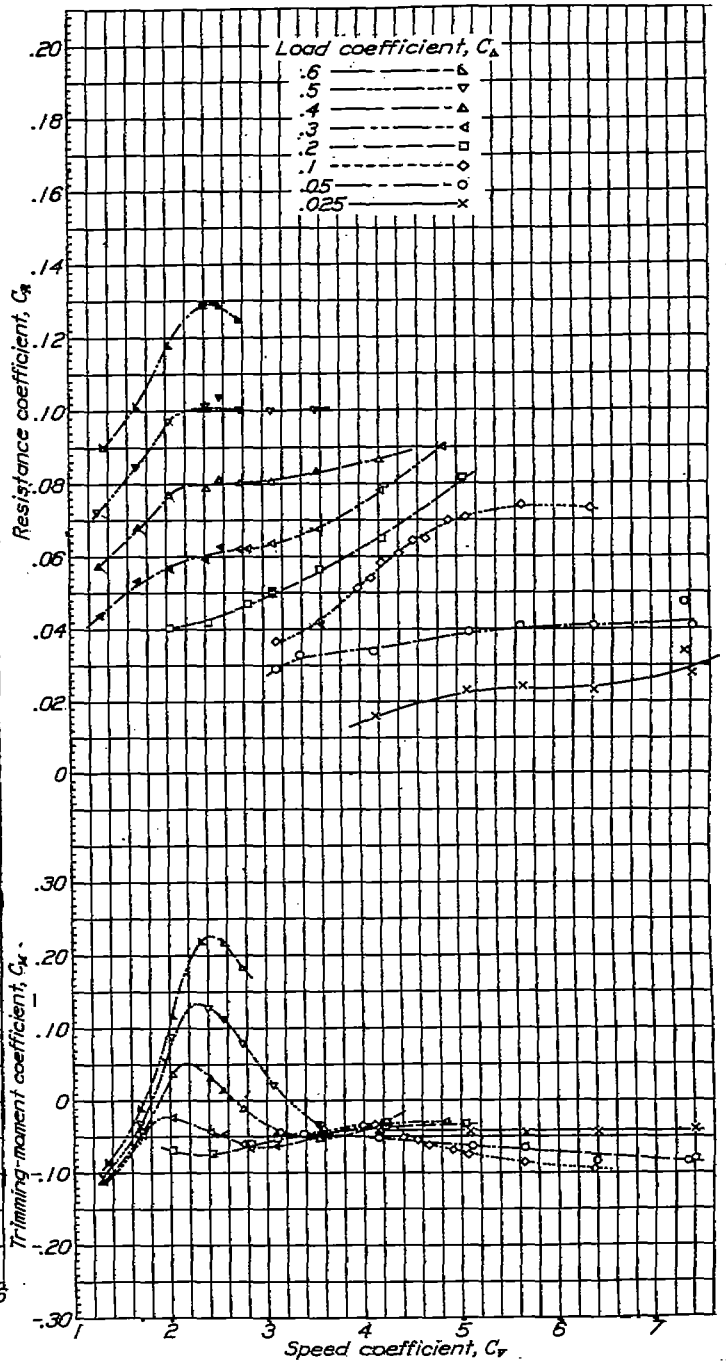

Figure 9.- Model 83A. Resistance and trimming-moment coefficients, $\tau=8^\circ$.

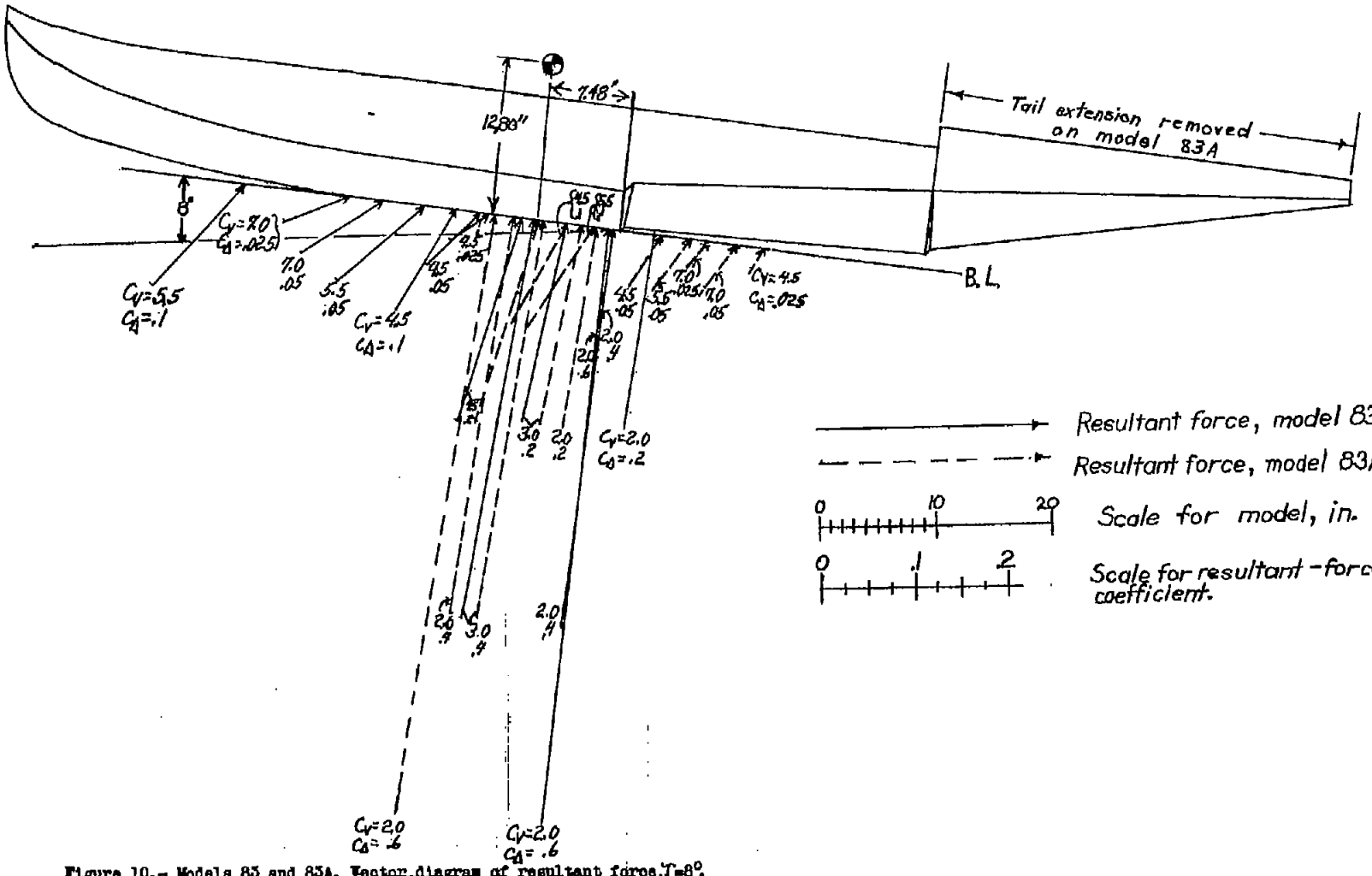

Figure 10.- Models 83 and 83A. Vector diagram of resultant force, $\gamma = 8°$. Resultant-force coefficient = $\sqrt{C_A^2 + C_R^2}$; direction of resultant force, $\delta = \tan^{-1} A/R$; beam of model, b = 17.72 inches.

Fig. 10